Human Molecular Genetics, 2009, Vol. 18, No. 16 **3098–3109**
doi:10.1093/hmg/ddp251
Advance Access published on May 28, 2009

Aberrant *de novo* methylation of the *p16^{INK4A}* CpG island is initiated post gene silencing in association with chromatin remodelling and mimics nucleosome positioning

Rebecca A. Hinshelwood[1], John R. Melki[2], Lily I. Huschtscha[3], Cheryl Paul[1], Jenny Z. Song[1], Clare Stirzaker[1], Roger R. Reddel[3,4] and Susan J. Clark[1,*]

[1]Cancer Program, Garvan Institute of Medical Research, 384 Victoria St, Darlinghurst, NSW 2010, Australia, [2]Human Genetic Signatures, PO Box 184, North Ryde, NSW 1670, Australia, [3]Children's Medical Research Institute, 214 Hawkesbury Rd, Westmead, NSW 2145, Australia and [4]University of Sydney, NSW 2006, Australia

Received February 26, 2009; Revised April 21, 2009; Accepted May 21, 2009

Changes in the epigenetic landscape are widespread in neoplasia, with *de novo* methylation and histone repressive marks commonly enriched in CpG island associated promoter regions. DNA hypermethylation and histone repression correlate with gene silencing, however, the dynamics of this process are still largely unclear. The tumour suppressor gene *p16^{INK4A}* is inactivated in association with CpG island methylation during neoplastic progression in a variety of cancers, including breast cancer. Here, we investigated the temporal progression of DNA methylation and histone remodelling in the *p16^{INK4A}* CpG island in primary human mammary epithelial cell (HMEC) strains during selection, as a model for early breast cancer. Silencing of *p16^{INK4A}* has been previously shown to be necessary before HMECs can escape from selection. Here, we demonstrate that gene silencing occurs prior to *de novo* methylation and histone remodelling. An increase in DNA methylation was associated with a rapid loss of both histone H3K27 trimethylation and H3K9 acetylation and a gradual gain of H3K9 dimethylation. Interestingly, we found that regional-specific 'seeding' methylation occurs early after post-selection and that the *de novo* methylation pattern observed in HMECs correlates with the apparent footprint of nucleosomes across the *p16^{INK4A}* CpG island. Our results demonstrate for the first time that *p16^{INK4A}* gene silencing is a precursor to epigenetic suppression and that subsequent *de novo* methylation initially occurs in nucleosome-free regions across the *p16^{INK4A}* CpG island and this is associated with a dynamic change in histone modifications.

INTRODUCTION

Widespread changes in genomic DNA methylation patterns occur during the transition from a normal cell to a cancer cell, and this is associated with chromatin remodelling and modified gene expression. Chromatin consists of nucleosomes, each containing 147 bp of DNA wrapped around an octamer of core histone proteins, which are separated from each other by ~50 bp of linker DNA (1). Nucleosome occupancy along DNA promoters plays an important role in transcriptional regulation (2), where both sliding and loss of nucleosomes affect the accessibility of the DNA to transcription factors (reviewed in 3). Malignant cells are characterized by a global reduction in genomic DNA methylation and a localized increase in methylation of CpG island-associated promoter regions (reviewed in 4–7). CpG islands have a frequency of CpG dinucleotides approximately five times greater than the genome, and commonly span the promoter region of ubiquitously expressed 'housekeeping' genes, and the 5′ or 3′ regions of many tissue-specific genes (8,9). Typically the CpG islands of transcriptionally active genes in normal cells are unmethylated and associated with permissive histone marks, whereas the CpG islands of transcriptionally inactive genes in cancer cells are densely methylated and associated

*To whom correspondence should be addressed. Tel: +612 92958315; Fax: +612 92958316; Email: s.clark@garvan.org.au

with repressive histone marks. However, the dynamics of aberrant *de novo* methylation in CpG island-associated promoters that mediate the transition from the unmethylated, active state to the densely methylated, inactive state remain largely unknown (10,11). It is not easy to address this question in tumour tissue because DNA hypermethylation is often an early event and therefore once the tumour is large enough to detect the aberrant methylation process has already occurred and the hypermethylated genes are already silenced.

In this study, we investigated the temporal change in epigenetic modifications in the CpG island of the $p16^{INK4A}$ gene (also known as CDKN2A and MTS-1). The $p16^{INK4A}$ protein binds and inhibits the activities of cyclin-dependent kinases CDK4 and CDK6 resulting in the hypophosphorylated form of pRb which acts as an inhibitor of cell-cycle progression (reviewed in 12). Many human tumour cell lines and primary tumours have lost expression of wild-type $p16^{INK4A}$ and this has led to the suggestion that the $p16^{INK4A}$ gene encodes a tumour suppressor (13). Indeed, the $p16^{INK4A}$ CpG island promoter is often hypermethylated in many tumours including breast tumours, and this appears to occur early in the oncogenic pathway (14–16). We and others have shown that loss of $p16^{INK4A}$ expression in human mammary epithelial cells (HMECs) is necessary for *in vitro* lifespan extension (17), and this also correlates with hypermethylation of the CpG island promoter (18–23). HMECs, when cultured in serum-free medium, exhibit two phases of growth (24,25). The first growth phase lasts for several population doublings (PDs), after which growth temporarily ceases (termed selection or M_0). Within 2–4 weeks, colonies of small cells with a basal mammary epithelial phenotype (26,27) appear with enhanced growth capacity and these colonies continue to proliferate for another 20–40 PDs before entering a second growth plateau resembling cell crisis, termed agonescence (28). HMECs isolated during the first growth phase are termed pre-selection cells, and those isolated during the second growth phase are termed either post-selection or variant HMECs (vHMECs) (19,22,24). Post-selection HMECs have been shown to share many characteristics of pre-malignant breast-cancer cells, including both genetic and epigenetic lesions (21,23,29,30), and therefore provide an ideal primary cell model to study early epigenetic changes in malignancy.

To investigate the temporal relationship between gene silencing, DNA methylation and chromatin remodelling, we analysed in detail *de novo* methylation of the $p16^{INK4A}$ CpG island in post-selection HMECs that were not expressing $p16^{INK4A}$. Using this primary tissue model, we first found that hypermethylation of the $p16^{INK4A}$ CpG island occurs only after the gene is silenced, and secondly we demonstrated that a low level of *de novo* methylation is associated with a dynamic remodelling of associated chromatin, as early as the first passage following selection. Lastly, we demonstrated that individual post-selection strains share a common pattern of regional-specific initial 'seeding' methylation within the $p16^{INK4A}$ CpG island. Using a high-resolution foot-printing technique, known as methylase-based single-promoter analysis assay (MSPA) (31), which exploits the fact that nucleosomes and binding factors restrict M. *Sss* I CpG methylase from methylating the DNA (32), we found that the 'seeding' methylation 'hot spots' correlated with the position of nucleosomes in the post-selection HMECs. Our results demonstrate for the first time that $p16^{INK4A}$ gene silencing is a precursor to epigenetic changes in post-selection HMECs and that subsequent *de novo* methylation occurs primarily in nucleosome-free regions across the $p16^{INK4A}$ CpG island and then progressively spreads to adjacent regions with proliferation.

RESULTS

$p16^{INK4A}$ is inactivated and heterogeneously methylated in post-selection HMECs

To study the underlying epigenetic changes that occur during $p16^{INK4A}$ silencing in HMECs that have undergone selection, we first used quantitative reverse transcription-PCR (qRT–PCR) to show that $p16^{INK4A}$ mRNA expression is inactivated, or down regulated, in the individual post-selection HMECs strains, Bre-12 and Bre-40 (30), and Bre-56, Bre-60 and Bre-80, compared with their isogenic pre-selection HMECs (Fig. 1A). We also confirmed that a loss of $p16^{INK4A}$ mRNA expression correlates with a loss in $p16^{INK4A}$ protein expression in Bre-56 and Bre-80 post-selection cells (Fig. 1B), as previously shown in Bre-40, Bre-60, Bre-70 and Bre-80 post-selection cells (19). Using direct PCR bisulphite sequencing, we reported that $p16^{INK4A}$ silencing in Bre-40, Bre-60, Bre-70 and Bre-80 post-selection HMECs correlates with extensive DNA hypermethylation of the CpG island-associated $p16^{INK4A}$ promoter (19). To better understand the dynamics and initial events leading to CpG island methylation, we have analysed the DNA methylation profiles in more detail by bisulphite clonal sequencing across three neighbouring regions of the $p16^{INK4A}$ CpG island spanning 1035 bp across the start of transcription and first exon (Supplementary Material, Fig. S1). The post-selection HMECs from each strain comprised 10–40 independent colonies that escaped selection and these colonies were pooled prior to analysis to gain a comprehensive view of the DNA methylation patterns. Figure 2 summarizes the bisulphite methylation sequencing data from Bre-38 and Bre-40 pre- and post-selection cells across 71 CpG sites (numbered from −19 CpG to +52 CpG relative to the start of transcription). The actively $p16^{INK4A}$ expressing pre-selection cells (Bre-38 and Bre-40) were essentially unmethylated from CpG sites −19 to +38, even though there was evidence of low-level sporadic CpG methylation noted in Bre-40 (Fig. 2A and C). In the pre-selection cells, the level of methylation was further enriched downstream from the start of transcription at CpG sites +40 to +52 in both Bre-38 and Bre-40 (Fig. 2A and C) correlating to the boundary region of the $p16^{INK4A}$ CpG island (Supplementary Material, Fig. S1). In contrast, in the corresponding Bre-38 and Bre-40 post-selection HMECs [passage 11 (p11) and 10 (p10), respectively] there was extensive DNA methylation across the three regions analysed (Fig. 2B and D) and this occurred in nearly all molecules, suggesting that DNA methylation of $p16^{INK4A}$ is bi-allelic.

Even though the DNA methylation was generally extensive, there was also considerable heterogeneity noted, with some molecules having no DNA methylation or methylation at only a few of the CpG sites, despite $p16^{INK4A}$ expression

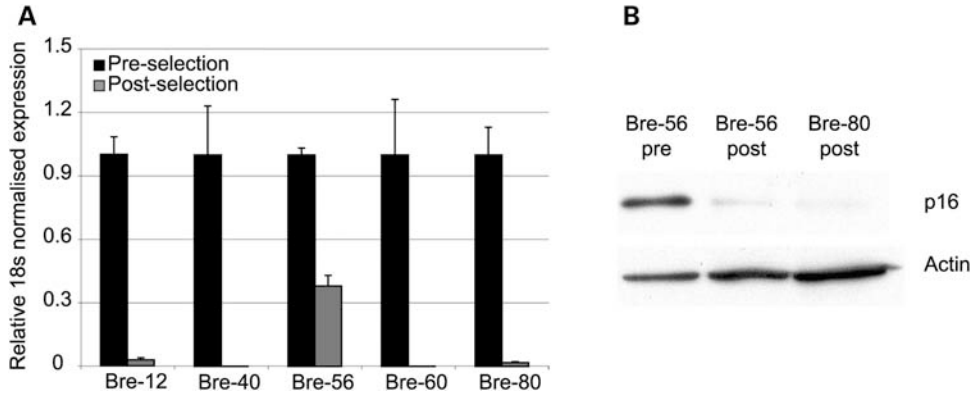

Figure 1. Suppression of *p16*^{INK4A} expression in post-selection HMECs. (**A**) mRNA levels of *p16*^{INK4A} in Bre-12, Bre-40, Bre-56, Bre-60 and Bre-80 post-selection HMECs were determined by quantitative RT–PCR. After normalizing expression to 18S rRNA, the fold change in expression levels was made relative to pre-selection HMECs. All donor post-selection strains show reduced levels of *p16*^{INK4A} mRNA. (**B**) Western blot showing p16^{INK4A} protein expression in Bre-56 pre-selection cells, and p16^{INK4A} silencing in Bre-56 and Bre-80 post-selection cells. Actin levels were used as a loading control.

being suppressed in these cells. The DNA methylation was also not uniformly distributed between the CpG sites. Blocks of adjacent CpG sites appeared to be more resistant to methylation, whereas other CpG sites appeared to be predominately methylated in 'hot spots' (Fig. 2B and D). Four such 'hot spots' were found to occur in similar locations in Bre-38 and Bre-40 post-selection HMECs across regions I and II. To ascertain whether the same CpG sites were also 'hot spots' for the *de novo* methylation in different post-selection HMEC strains, we further analysed region II in other post-selection HMEC strains, Bre-60 (p7) and Bre-70 (p9) (Fig. 3). Focal 'hot spots' of methylation of adjacent CpG sites were also observed for these post-selection HMECs, even though the location of the specific sites were slightly different from strain to strain.

p16^{INK4A} silencing in post-selection HMECs occurs prior to DNA hypermethylation

We previously showed that *p16*^{INK4A} is inactivated and methylated in post-selection HMECs (19), but what was not clear at the time was if DNA methylation was causing *p16*^{INK4A} silencing or if *p16*^{INK4A} silencing was promoting DNA methylation. The fact that the methylation pattern in all the different post-selection HMEC strains was heterogeneous, and a number of molecules remained unmethylated or had only minimal methylation in the early passages after selection (Figs 2B,D and Fig. 3), led us to ask if *p16*^{INK4A} silencing preceded DNA methylation. To address this question, we used laser capture microscopy to isolate individual post-selection HMECs that had just emerged from selection and stained negative for *p16*^{INK4A} expression (Fig. 4A–C). At this early time point, each post-selection colony had only expanded to approximately 30 cells or 4–5 PDs. We performed bisulphite sequencing on pools of 20 individually laser-captured cells that were negative for *p16*^{INK4A} expression from a colony at the time of selection (Fig. 4B), and compared the methylation profile to 20 pooled individually laser-captured pre-selection or senescent cells, from the same dish, that were positive for *p16*^{INK4A} expression (Fig. 4A, Supplementary Material, Fig. S2). Figure 4D summarizes the methylation results and shows that there was little or no methylation evident in either the *p16*^{INK4A} silent HMECs at the time of selection, or the surrounding *p16*^{INK4A} expressing pre-selection cells (Fig. 4D). The silencing of the *p16*^{INK4A} gene therefore appears to occur independently and prior to subsequent *de novo* methylation.

p16^{INK4A} hypermethylation originates from focal CpG sites and progressively spreads with proliferation

We performed a detailed analysis on post-selection cells derived from a single HMEC colony to ascertain if the heterogeneity in DNA methylation observed in post-selection HMECs was due to the fact that we had pooled individual colonies prior to passaging or if the heterogeneity reflected the inherent stochastic nature of *de novo* and or maintenance methylation. We isolated HMECs from a single Bre-80 colony at selection and cultured the cells for an additional 39 passages and analysed methylation at passages 1, 4, 10, 23, 26 and 39. Figure 5 shows the progressive expansion of DNA methylation we observed across region II of the *p16*^{INK4A} CpG island. In the pre-selection Bre-80 cells, region II was essentially unmethylated with only a few single methylated CpG sites; however, by passage 1 after selection, 'hot spots' of methylation were already observed in some of the molecules. With increasing passage number, the density of methylation also progressively increased, and by passage 39 all molecules were hypermethylated in nearly 50% of CpG sites, with two discrete 'hot spots' flanking a region of CpG sites that was more resistant to methylation. Indeed, the overall methylation pattern generated from the single Bre-80 clone was remarkably similar to the patterns observed from the pooled post-selection colonies in each of different HMEC strains (for example Bre-60 and Bre-70) (Fig. 5B), suggesting a directive process.

Nucleosome occupancy of the *p16*^{INK4A} CpG island mimics the post-selection HMEC methylation profile

The regularity of methylation 'hot spots' that we observed across the *p16*^{INK4A} CpG island, in each of the different

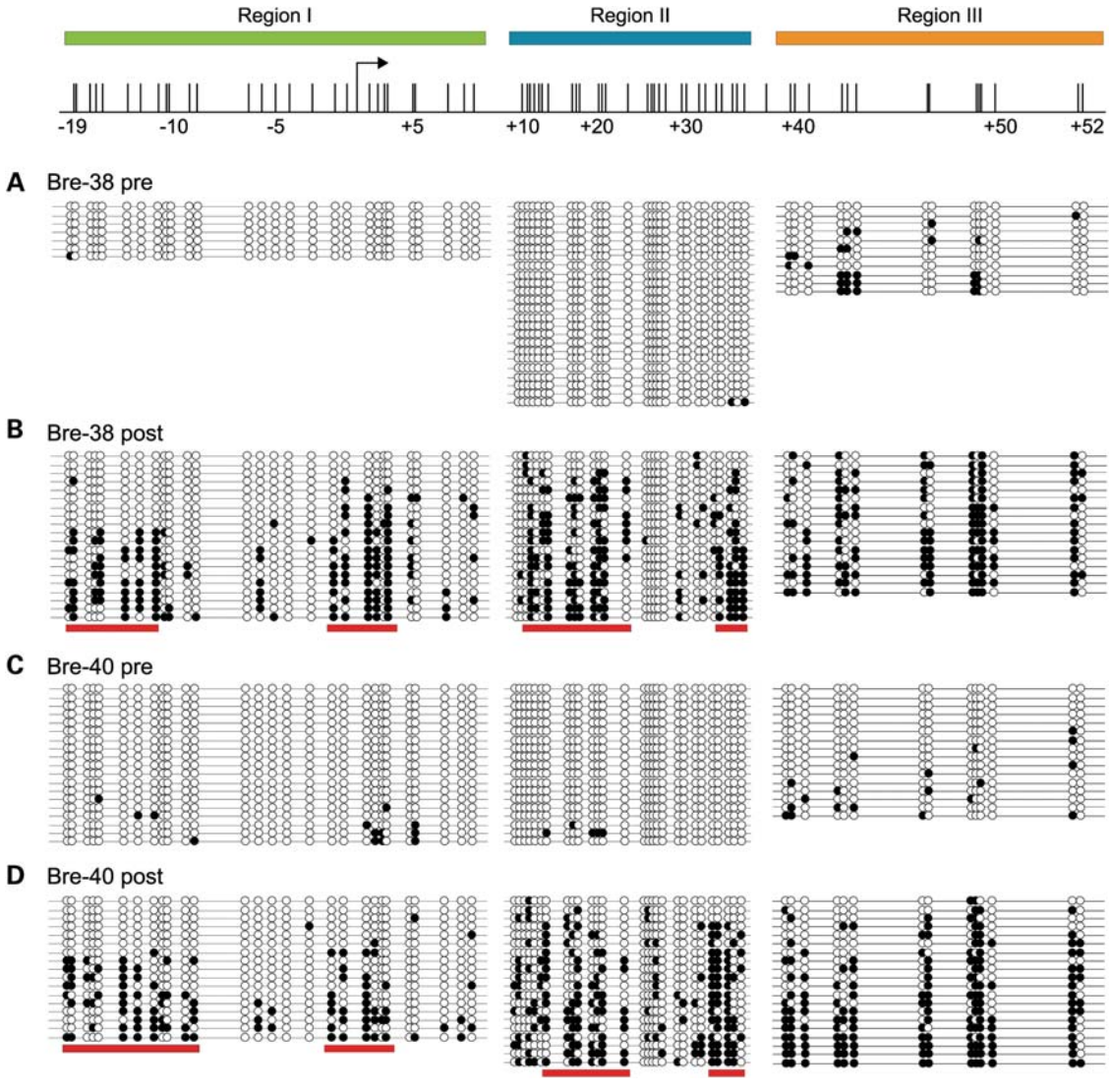

Figure 2. *p16*^{INK4A} silencing in post-selection cells is accompanied by DNA hypermethylation. Bisulphite methylation clonal sequencing analysis was performed across three neighbouring regions of the *p16*^{INK4A} CpG island associated promoter region. Amplicon locations: region I, region II and region III. The start of transcription, as indicated by Genbank accession number *p16*^{INK4A} (AB060808), is indicated by a black arrow. CpG sites are numbered relative to the start of transcription. (**A**) Bre-38 pre-selection cells [passage 5 (p5)]. (**B**) Bre-38 post-selection cells (p11). (**C**) Bre-40 pre-selection cells (p5). (**D**) Bre-40 post-selection cells (p10). White circle, unmethylated CpG site; black circle, methylated CpG site. Red bars indicate focal 'hot spots' of DNA methylation in post-selection HMECs.

post-selection HMEC strains, prompted us to address if this signature correlates with the position of nucleosome repeat units. We used the new high-resolution foot-printing technique, known as MSPA (31), to determine the position of the nucleosomes across the three neighbouring regions of the *p16*^{INK4A} CpG island promoter. The advantage of this method is that it provides an *in vitro* map of regions that are protected from the DNA methyltransferase enzyme. Nuclei were prepared from Bre-38 pre-selection HMECs and analysed for accessibility to M. *Sss* I CpG methylase. M. *Sss* I CpG methylase treatment of control naked genomic DNA was also performed as a control for the extent of enzyme activity. Figure 6A confirms that *p16*^{INK4A} was essentially unmethylated in Bre-38 pre-selection HMECs and after M. *Sss* I treatment the control genomic DNA became extensively methylated (Fig. 6B). In contrast, when the Bre-38 pre-selection nuclei were treated with M. *Sss* I, the *p16*^{INK4A} DNA molecules were methylated in three distinct patterns (Fig. 6C). Class I clones, exhibited two focal regions of methylation flanking a central region of protection from M. *Sss* I treatment, whereas class II and III clones appeared to be protected from methylation at one or other end of the *p16*^{INK4A} amplicons examined. When the methylation pattern of the clones were analysed collectively from regions I, II and III, three discrete regions of $\sim$150 bp in length are shown to be more protected from M. *Sss* I treatment (Fig. 6D), consistent with the presence of three nucleosomes. However, in the region spanning the start of transcription, an extended region of *in vitro* M. *Sss* I methylation was observed, suggesting the loss of a nucleosome in the actively expressing Bre-38 pre-selection HMECs (Fig. 6D). Interestingly, the regions that were more susceptible to *in vitro* M. *Sss* I

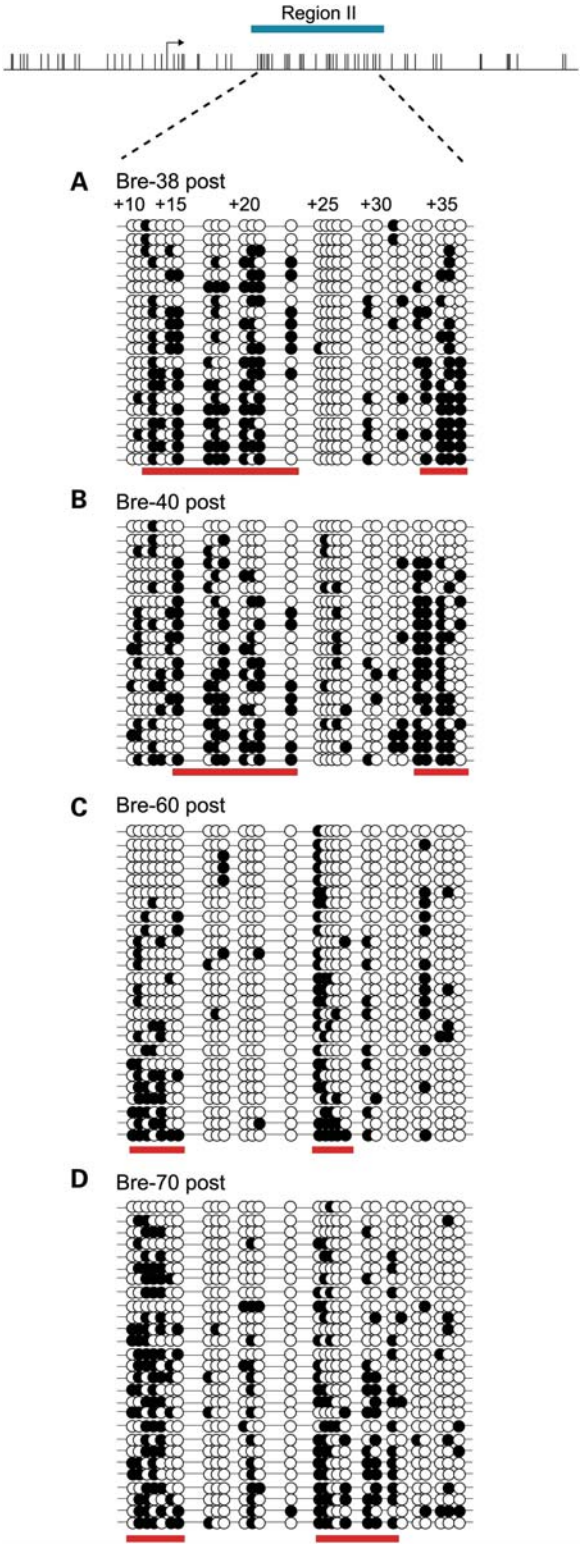

Figure 3. DNA hypermethylation of $p16^{INK4A}$ occurs at focal 'hot spot' regions. Bisulphite methylation clonal sequencing analysis was performed at region II of the $p16^{INK4A}$ CpG island-associated promoter, revealing that there is a distinct pattern of DNA methylation. CpG sites are numbered relative to the start of transcription. (**A**) Bre-38 post-selection cells (p11). (**B**) Bre-40 post-selection cells (p10). (**C**) Bre-60 post-selection cells (p7). (**D**) Bre-70 post-selection cells (p9). White circle, unmethylated CpG site; black circle, methylated CpG site. Red bars indicate focal 'hot spots' of DNA methylation.

methylation of Bre-38 nuclei, correspond in general to the wave signature pattern of methylation observed *in vivo* in the Bre-38 post-selection HMECs, as summarized in Figure 6E. Conversely, the regions that were protected from M. *Sss* I methylation *in vitro* (Fig. 6D) correspond to the regions protected *in vivo* in the Bre-38 post-selection HMECs (Fig. 6E). In both cases, the region spanning the start of transcription was more susceptible to methylation, but in contrast to the *in vitro* M. *Sss* I methylation data, the *in vivo* methylation profile observed in the Bre-38 post-selection HMECs where $p16^{INK4A}$ expression was inactivated was more discrete, consistent with a gain of a nucleosome near the start of transcription (Fig. 6D,E). Supplementary Material, Figure S3 shows a comparative analysis of *in vitro* MSPA pre-selection Bre-38 data with the *in vivo* Bre-38 post-selection $p16^{INK4A}$ methylation patterns using lowess curves that were generated and smoothing applied over 10 data points. A clear correlation can be observed between the apparent nucleosome footprint generated using the MSPA technique and the DNA methylation wave signature pattern observed in the post-selection HMECs. However, after the start of transcription, the phasing of the methylation footprint, reflecting nucleosome positioning, appeared to be more compact in the post-selection cells, which is consistent with the inactive state of $p16^{INK4A}$ in these cells and *de novo* methylation in the nucleosome-free linker regions.

To determine if a similar nucleosome footprint was observed in breast-cancer cells, we performed MSPA on MDAMB453 cells, a breast-cancer cell line in which $p16^{INK4A}$ is also expressed and unmethylated. First, as for Bre-38 cells, regions I and II spanning the $p16^{INK4A}$ CpG island are essentially unmethylated in the expressing MDAMB453 cells (Supplementary Material, Fig. S4A). Secondly, when MDAMB453 nuclei were treated with M. *Sss* I, we also observed distinct focal regions of *in vitro* methylation in similar focal regions to the pre-selection Bre-38 M. *Sss* I treated nuclei (Supplementary Material, Fig. S4B). Thirdly, the M. *Sss* I methylation clonal pattern found in the MDAMB453 cells also mimics the *in vivo* wave pattern of methylation observed for the post-selection cells Bre-38 (Supplementary Material, Fig. S4C). The combined data supports the hypothesis that the nucleosome footprint dictates the *de novo* methylation signature pattern across the $p16^{INK4A}$ CpG island in both normal breast cells and breast-cancer cells.

$p16^{INK4A}$ epigenetic silencing in post-selection HMECs is associated with dynamic chromatin remodelling

To determine the relationship between $p16^{INK4A}$ silencing in post-selection HMECs, DNA methylation and chromatin remodelling, we performed chromatin immunoprecipitation (ChIP) assays with acetylated H3K9 (H3K9Ac), dimethylated H3K9 (H3K9Me2) and trimethylated H3K27 (H3K27Me3) antibodies to compare histone modifications in pre- and post-selection cells. $p16^{INK4A}$-associated chromatin isolated from actively expressing pre-selection HMECs was enriched for active H3K9Ac marks and rapid deacetylation was observed in the post-selection cells at the first passage after selection which remained deacetylated with further passaging (Fig. 7A). In contrast, $p16^{INK4A}$ associated chromatin from pre-selection HMECs was depleted in the repressive H3K9Me2 mark, but after selection slowly accumulated histone methylation marks over several

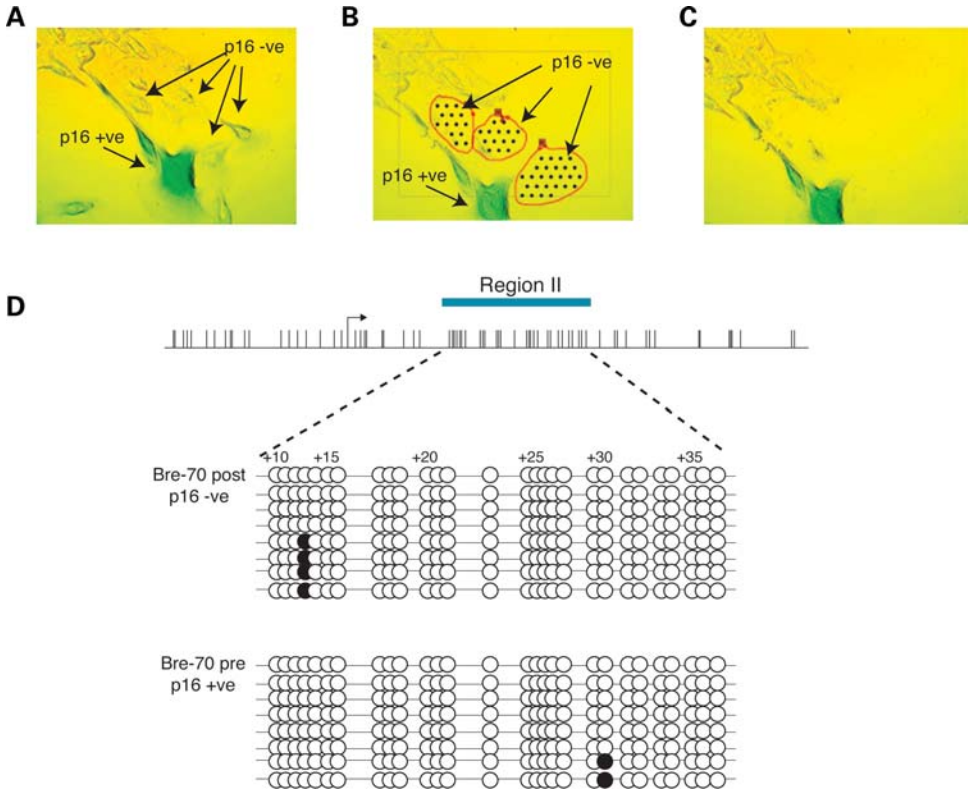

Figure 4. *p16*^{INK4} silencing in HMECs occurs prior to DNA hypermethylation. Laser capture dissection techniques were used to isolate single Bre-70 pre- and post-selection cells that were positive or negative for p16^{INK4A} expression. (**A**) Bre-70 pre-selection cells expressing p16^{INK4A} (positive staining) and small post-selection cells silenced for p16^{INK4A}. (**B**) Selection of p16^{INK4A} silenced cells for dissection. (**C**) Cells after dissection, showing specific isolation of p16^{INK4A} silenced cells. (**D**) Bisulphite methylation clonal sequencing analysis of *p16*^{INK4A} from single Bre-70 post-selection (*p16*^{INK4A} silenced) and pre-selection cells (*p16*^{INK4A} expressed) isolated by laser capture microscopy. Newly emerging post-selection HMECs that were negative for p16^{INK4A} did not exhibit methylation. CpG sites are numbered relative to the start of transcription. White circle, unmethylated CpG site; black circle, methylated CpG site.

passages (Fig. 7B). Interestingly, *p16*^{INK4A}-associated chromatin was also found to be enriched in the polycomb mark H3K27Me3 in pre-selection cells, and this was rapidly depleted in post-selection HMECs at the first passage after selection (Fig. 7C). Similar results were observed using different HMEC strains (Supplementary Material, Fig. S5). Together these data show that *p16*^{INK4A} silencing at selection promotes a progressive increase in *de novo* CpG methylation in post-selection HMECs (Fig. 7D) and a parallel deacetylation of H3K9 and loss of trimethylated H3K27, whereas dimethylation of H3K9 occurs subsequently and gradually increases with DNA methylation accumulation.

DISCUSSION

The results presented in this paper provide for the first time a comprehensive analysis of the temporal steps involved in *p16*^{INK4A} silencing, epigenetic reprogramming and nucleosome positioning in a model for early malignancy of breast cancer. HMECs isolated from disease-free breast tissue provide a uniquely informative system to study early events in breast tumourigenesis (reviewed in 33). Post-selection or variant HMECs exhibit many preneoplastic characteristics, including transcriptional silencing of the *p16*^{INK4A} tumour suppressor gene and overexpression of cyclo-oxygenase 2 (*Cox-2*) (18–23) as well as epigenetic deregulation of the TGF-β pathway (30). Epigenetic deregulation of *p16*^{INK4A} also occurs commonly in pre-malignant lesions and rare foci of morphologically normal epithelial cells exhibiting *p16*^{INK4A} methylation have been identified *in vivo* in disease-free breast tissue (22). It has been postulated that these foci are cancer precursors, which can promote malignancy with additional epigenetic and or genetic changes (29).

One of the biggest challenges in dissecting the processes involved in epigenetic reprogramming in cancer is that the changes occur early in oncogenesis and are consequently difficult to study in clinical samples. We therefore used HMECs grown in serum-free conditions to study the early epigenetic changes that are associated with *p16*^{INK4A} silencing. We and others have previously shown that *p16*^{INK4A} silencing in post-selection cells that arise under these culture conditions is associated with DNA hypermethylation of the CpG island promoter and this occurs just as the first post-selection cells emerge from selection (18–23). We now demonstrate that DNA hypermethylation of *p16*^{INK4A} CpG island occurs only after the gene is silent and that the initial 'seeds' of *de novo* methylation accumulate in the accessible regions of the chromosome and this is associated with a dynamic remodelling of the chromatin.

Over the years, there has been constant debate over the mechanism of epigenetic silencing of tumour suppressor genes in cancer (11,34,35). Central to this debate is the

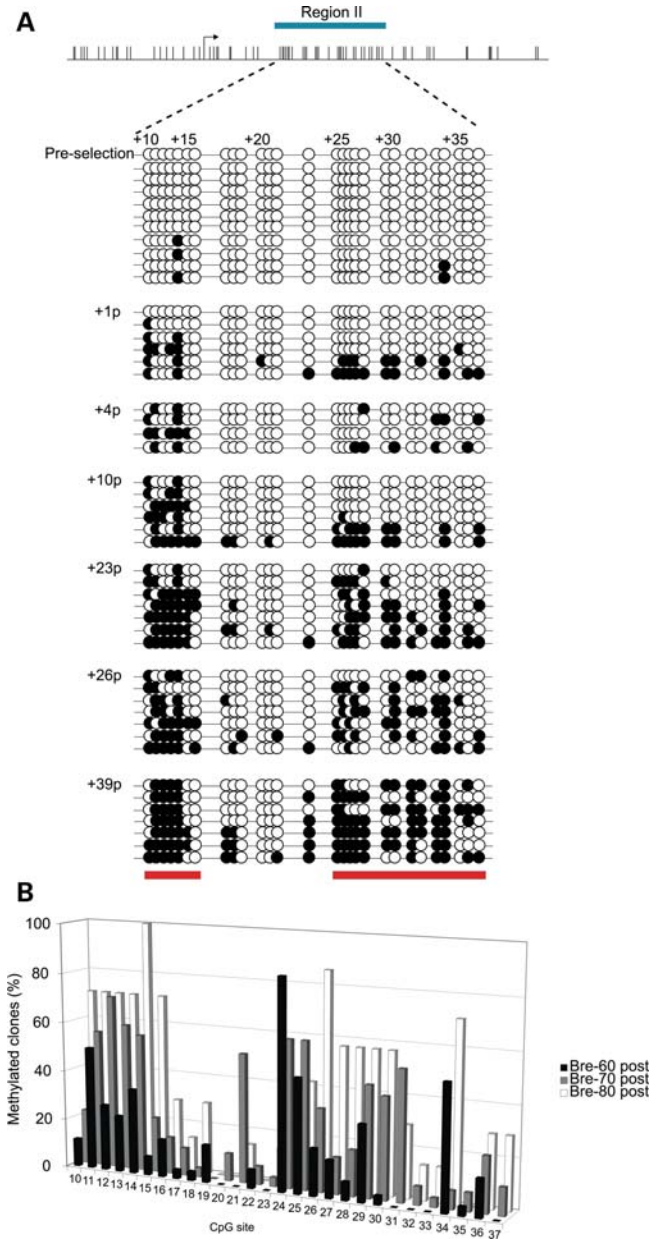

Figure 5. DNA hypermethylation of $p16^{INK4A}$ in a single Bre-80 colony increases and expands with successive passaging. (**A**) Bisulphite methylation clonal sequencing analysis of $p16^{INK4A}$ in a single Bre-80 colony at selection (top panel). A single Bre-80 colony was cultured until the end of its lifespan, and the DNA methylation status of $p16^{INK4A}$ determined at passage numbers 1, 4, 10, 23, 26 and 39 (relative to selection). Density of methylation of the CpG sites increases with increasing passage number. CpG sites are numbered relative to the start of transcription. White circle, unmethylated CpG site; black circle, methylated CpG site. Red bars indicate focal 'hot spots' of DNA methylation. (**B**) Quantitation of bisulphite clonal sequencing data for Bre-60 (p7), Bre-70 (p9) and Bre-80 (p23) post-selection cells, highlighting similar methylation patterns.

question of whether DNA methylation and histone modifications are a consequence or cause of gene silencing? A favoured dogma is that DNA methylation causes gene silencing and was demonstrated in early *in vitro* studies (36–38). However, more recently the hypothesis that DNA methylation is a consequence of gene silencing is gaining support. We have previously reported that transcriptional silencing of a genetically manipulated *GSTP1* gene in LNCaP cells precedes DNA methylation (39), and the low level 'seeding' methylation observed in normal cells promotes H3K9 deacetylation and H3K9 methylation. In contrast, Bachman *et al*. 2003 (35) reported that silencing of $p16^{INK4A}$ and H3K9 methylation preceded DNA methylation also using an experimentally contrived situation. The advantage of the HMEC system is that it allows us to address the interplay between gene inactivation and epigenetic changes at the earliest time points after $p16^{INK4A}$ silencing in an *in vivo* setting. Using laser capture dissection of single cells clearly demonstrated that *de novo* methylation occurred post gene silencing, and analysis of a single colony showed that methylation was progressive rather than being a single aberrant event that encompasses the entire island, supporting previous findings (10,19). Even though the methylation of individual CpG sites was stochastic, it was clear that there was an overall similar pattern between different HMEC strains. Using the new single-molecule footprinting technique developed to visualize nucleosome occupancy at high resolution (31), we were able to demonstrate that the signature wave pattern of methylation observed in the post-selection cells was similar to the observed nucleosome footprint across the $p16^{INK4A}$ CpG island. Our results suggest that chromatin accessibility is dictating the initial access to the DNA methyltransferase enzyme, thereby only permitting aberrant *de novo* methylation to limited regions within the $p16^{INK4A}$ CpG island which then spreads progressively with PD. Our data also suggests that the nucleosomes are quite mobile in the actively expressing cells, and not precisely positioned along the $p16^{INK4A}$ promoter. This is not unexpected, as it is well known that nucleosomes are not a simple static unit; rather, they are a dynamic element that can slide along the DNA, thus permitting access or constraints to transcriptional machinery (3). Indeed, the transitory nature of nucleosomes was emphasized in a recent MSPA analysis of the *GRP78* promoter during endoplasmic reticulum (ER) stress (40). Similar to our finding, silent promoters have generally been shown to be enriched for nucleosomes relative to their active counterparts (41), and nucleosome depletion at CpG islands has been described for several epigenetically regulated human gene promoters (31,42). For example, the methylated and silent *MLH1* promoter was found to be occupied by three nucleosomes in RKO cells, which were evicted upon demethylation and activation of the promoter by 5-aza-2'-deoxycytidine (42).

The final implication of our work relates to chromatin remodelling that occurred in parallel with the *de novo* methylation. As summarized in Fig. 8, we found the $p16^{INK4A}$ CpG island in pre-selection cells was associated with the lack of a nucleosome at the start of transcription and bivalent histones consisting of the active H3K9Ac mark and the repressive polycomb EZH2-associated H3K27Me3 mark. After $p16^{INK4A}$ inactivation, the nucleosomes are remodelled with the gain of a nucleosome across the start of transcription, and a rapid deacetylation of H3K9 in concert with the rapid removal of the H3K27Me3 polycomb mark. In contrast, dimethylation of H3K9 accumulates more gradually in parallel with the accumulation of DNA methylation, resulting in consolidation of $p16^{INK4A}$ gene silencing. Our data supports recent findings

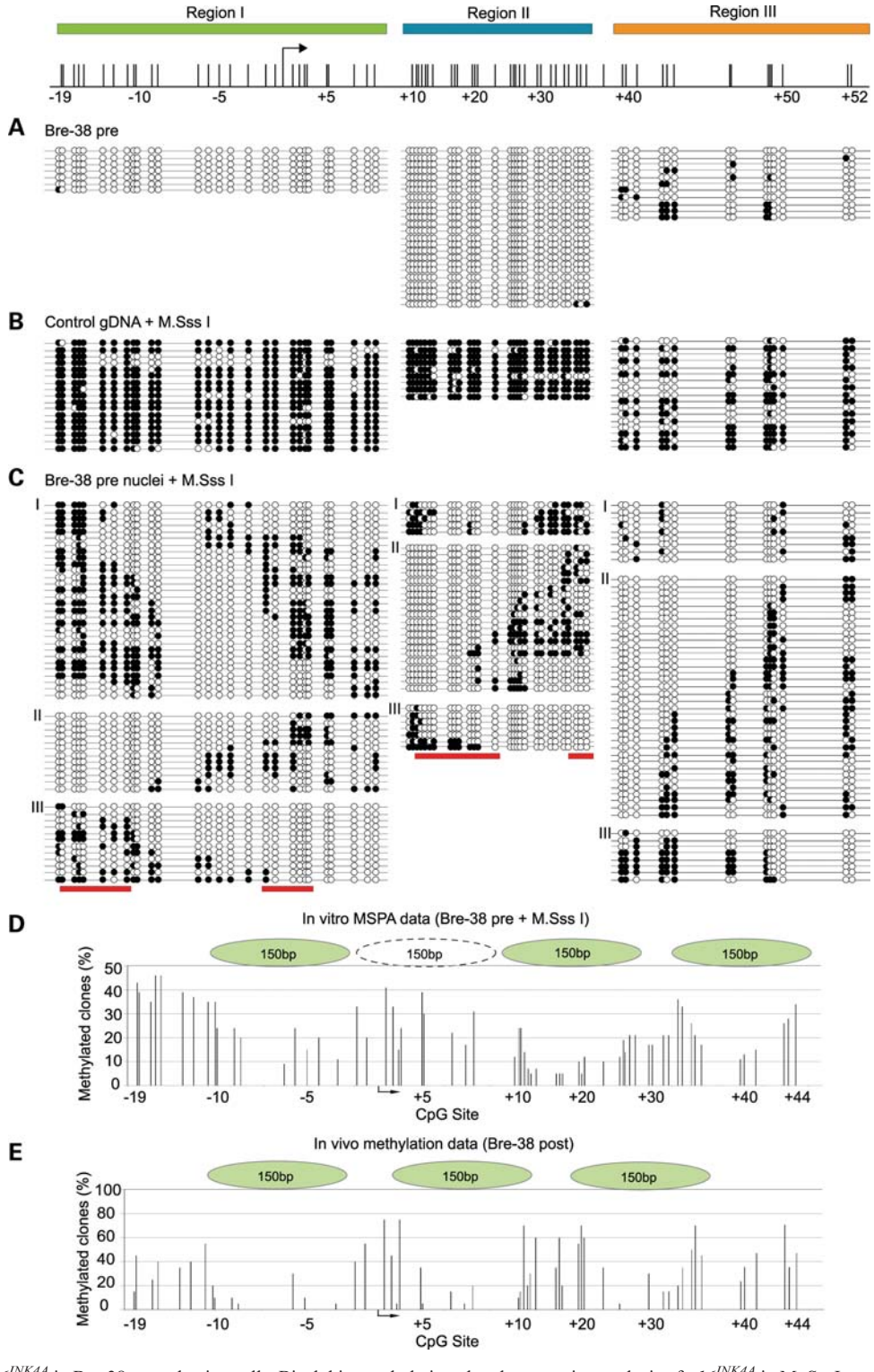

Figure 6. MSPA of *p16*^{INK4A} in Bre-38 pre-selection cells. Bisulphite methylation clonal sequencing analysis of *p16*^{INK4A} in M. *Sss* I treated Bre-38 pre-selection cells was performed to ascertain whether nucleosomes influence *p16*^{INK4A} methylation patterns in post-selection HMECs. (**A**) Untreated Bre-38 pre-selection cells. (**B**) M. *Sss* I treated control genomic DNA. (**C**) M. *Sss* I treated Bre-38 pre-selection nuclei. Methylation patterns were divided into three distinct classes; class I (top), class II (middle) and class III (bottom). (**D**) Quantitation of *in vitro* Bre-38 M. *Sss* I MSPA clonal data. (**E**) Quantitation of *in vivo* Bre-38 post-selection clonal methylation data from Fig. 2B. The methylation footprints at the single molecule level reveal ∼150 bp protected regions consistent with nucleosome units across each of the three regions. Proposed nucleosome units (∼150 bp) are indicated by green ovals, while nucleosome devoid regions are indicated by dotted white ovals. CpG sites are numbered relative to the start of transcription. White circle, unmethylated CpG site; black circle, methylated CpG site. Red bars indicate focal 'hot spots' of DNA methylation in Bre-38 post-selection cells (as shown in Fig. 2B).

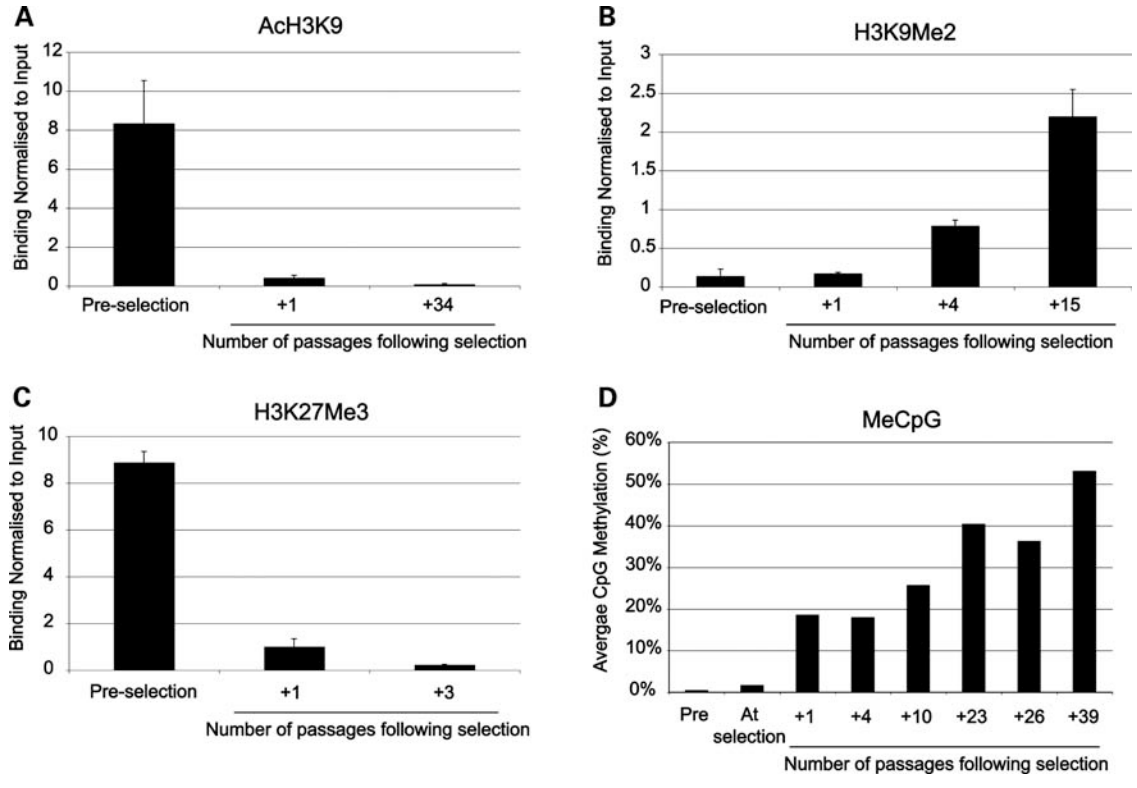

Figure 7. Interplay between accumulation of repressive chromatin and *de novo* CpG methylation associated with $p16^{INK4A}$ epigenetic silencing. Chromatin from pre- and post-selection HMECs was immunoprecipitated with (**A**) acetylated H3K9 (H3K9Ac), (**B**) dimethylated H3K9 (H3K9Me2) and (**C**) trimethylated H3K27 (H3K27Me3) antibodies. The amount of immunoprecipitated DNA (relative binding) was quantified by real-time PCR and was calculated as a ratio of immunoprecipitated DNA to the total amount of input. (**D**) Bisulphite clonal sequencing data for Bre-80 (as described in Fig. 5) was quantitated as average CpG methylation at each passage. A rapid deacetylation of H3K9 was associated with a loss of H3K27me3 and gain of DNA methylation followed by a slower gain of H3K9 methylation.

that many genes including those involved in cell-fate determination, stem-cell renewal, cell growth and cell division are marked by polycomb in the normal cells, but are susceptible to aberrant DNA methylation in cancer cells (43,44). What remains unclear is the mechanism responsible for rapid change from the bivalent histone mode to one associated with DNA methylation and histone deacetylation and methylation. Our studies demonstrate that gene silencing in pre-malignancy is key to tipping the balance from an epigenetically plastic condition to one that becomes repressively locked.

MATERIALS AND METHODS

Cells and cell culture

Breast tissue removed from reduction mammoplasties was obtained with institutional Ethics Committee approval and informed donor consent. HMEC cultures were prepared from normal breast tissue for donor strains Bre-12, Bre-38, Bre-40, Bre-56, Bre-60, Bre-70 and Bre-80 as previously described (19,30). The pre-selection and post-selection HMECs were subcultured according to the protocol described in (19,24).

Quantitative real-time reverse transcription PCR

RNA was extracted from Bre-12, Bre-40, Bre-56, Bre-60 and Bre-80 pre- and post-selection HMECs using Trizol Reagent (Invitrogen, Carlsbad, CA, USA) according to the manufacturer's protocol. cDNA was reverse transcribed from 1 μg of total RNA using SuperScript III RNase H^- Reverse Transcriptase (Invitrogen) according to the manufacturer's protocol. The reaction was primed with 150 ng of random primers (Boehringer-Mannheim, Castle Hill, NSW, Australia). The reverse transcription reaction was diluted 1:10 with sterile H_2O before addition to the reverse transcription PCR. $p16^{INK4A}$ expression primer sequences are described in Supplementary Material, Table S1. $p16^{INK4A}$ expression was quantitated using the 7900HT Applied Biosystems Sequence Detection System as described (30).

Western blotting

Western blot analysis using Bre-56 pre- [passage 4 (p4)] and post-selection (p12), and Bre-80 post-selection (p52) cells was performed essentially as described in (45). $p16^{INK4A}$ was detected with an anti-p16 (Ab-1) mouse monoclonal antibody (DSC-50.1/H4: Calbiochem/Merck KGaA, Darmstadt, Germany).

DNA isolation

DNA was isolated from less than 1×10^6 pre- and post-selection cells using simple lysis buffer (2 μg tRNA, 280 ng/μl proteinase K, 1% SDS) (46), or from $1–3 \times 10^6$ cells using either Puregene DNA isolation kit (Gentra Systems, Inc., Minneapolis, USA) according to the manufacturer's instructions,

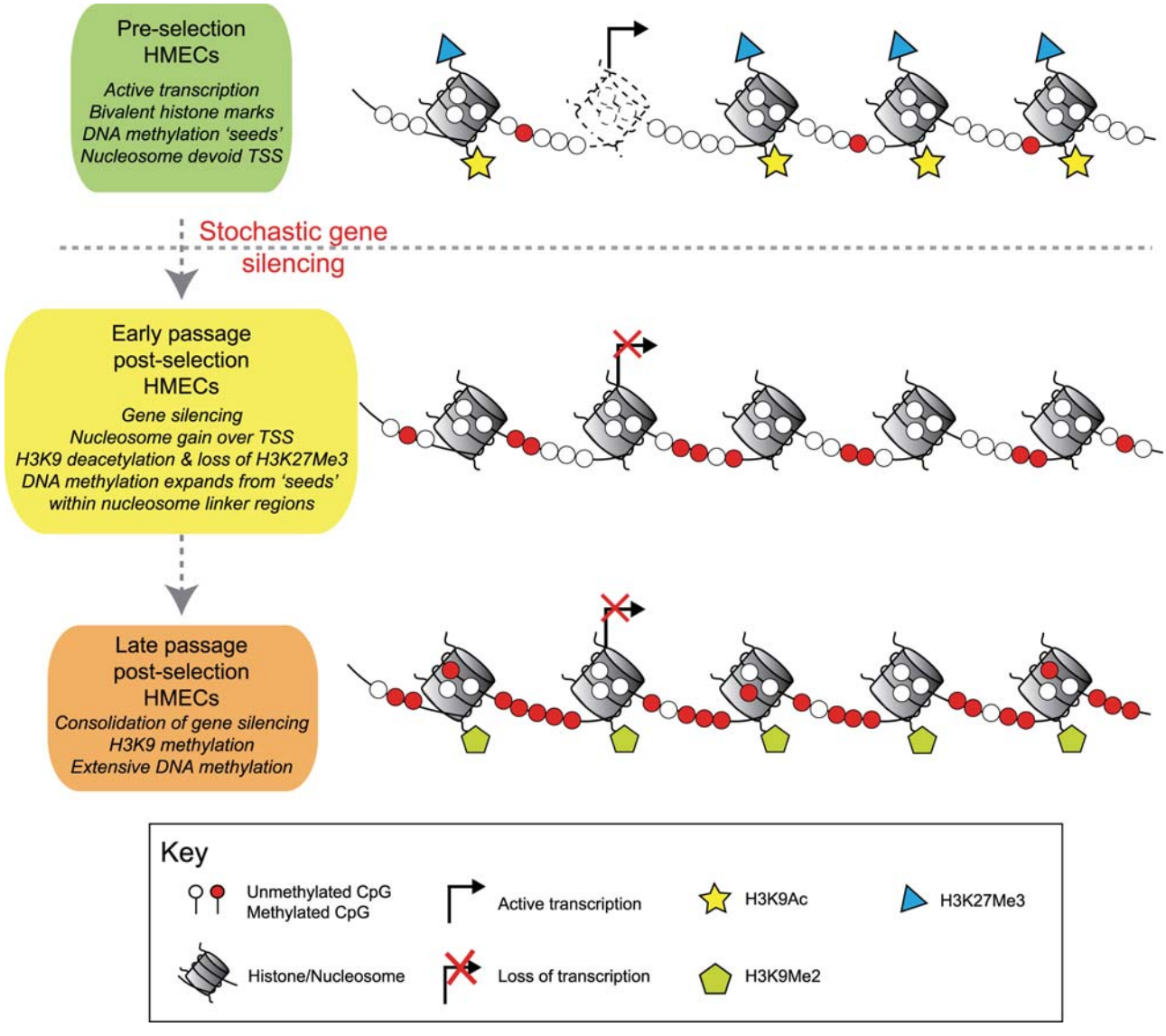

Figure 8. Summary of epigenetic silencing of $p16^{INK4A}$ in post-selection HMECs. In pre-selection HMECs, the $p16^{INK4A}$ transcription start site (TSS) is devoid of a nucleosome. The CpG island-associated promoter region is marked by DNA methylation 'seeds', there is active gene transcription and the chromatin is in a bivalent state as it is marked by both active (H3K9Ac) and repressive (H3K27Me3) histone modifications. As a consequence of stochastic gene silencing, $p16^{INK4A}$ undergoes epigenetic deregulation in post-selection HMECs through a DNA methylation-associated mechanism. In early post-selection cells, there is nucleosome gain across the TSS, which is accompanied by loss of H3K27Me3, deacetylation of H3K9, and evidence of DNA methylation expansion from 'seeds' within nucleosome linker regions. In late passage post-selection HMECs, there is consolidation of gene silencing through an enrichment of H3K9Me and extensive spreading and accumulation of DNA methylation.

or with Trizol Reagent with the following modifications to the manufacturer's protocol: 300 μl of 100% ethanol and 20 μg of tRNA was added to the reserved organic phase, the samples inverted and incubated at room temperature for 3 min. Samples were centrifuged at 12 000 g for 15 min at 4°C. The supernatant was carefully removed, the DNA pellet resuspended in 18 μl of simple lysis buffer and the sample incubated at 55°C overnight prior to bisulphite conversion.

Laser capture microdissection

HMECs were stained for $p16^{INK4A}$ expression with a Envision DAKO kit as previously described (19). Single pre-selection Bre-70 cells that stained $p16^{INK4A}$ positive and post-selection Bre-70 cells that were $p16^{INK4A}$ negative, were isolated using the PALM Robot Microbeam laser microdissection system (P.A.L.M GmbH, Bernried, Germany) (47). Twenty cells for each cell type were captured in the tube cap in duplicate for two separate experiments and placed in 18 μl lysis buffer (100 mM Tris–HCl pH 8.0, 3% SDS, 50 mM EDTA, 200 μg/ml Proteinase K).

DNA methylation studies

Bisulphite genomic sequencing was used to analyse the methylation status of three neighbouring regions of $p16^{INK4A}$ in pre- and post-selection HMECs (Supplementary Material, Fig. S1). The bisulphite reaction was carried out on extracted

DNA for 16 h at 55°C on up to 2 μg of digested DNA, under conditions described previously (48,49). Laser-captured cells were incubated in 18 μl of DNA lysis buffer for 30 mins at 37°C prior to bisulphite treatment for 4 h, as described (49). After bisulphite conversion, the DNA was ethanol precipitated, dried, resuspended in 10–50 μl H_2O and stored at −20°C. Triplicate PCR amplifications were performed for $p16^{INK4A}$ and pooled. The primer sequences and location of the $p16^{INK4A}$ amplicons in relation to the CpG island and start of transcription are summarized in Supplementary Material, Table S1 and Supplementary Material, Figure S1. The methylation status of $p16^{INK4A}$ was determined by bisulphite clonal sequencing of the pooled PCR products, as described (50) to ensure representative clonal analysis. Example DNA sequence traces are shown in Supplementary Material, Fig. S6.

Methylase-based single-promoter analysis assays

Nucleosome positioning assays were performed by a high-resolution, MSPA, essentially as described in (31,42) and with the following modifications. Actively growing Bre-38 pre-selection HMECs, or MDAMB453 breast cancer cells, were trypsinized and washed twice with cold PBS. Cells were resuspended in 1 ml of cold RSB buffer (10 mM Tris–HCl; pH 7.4, 10 mM NaCl and 3 mM $MgCl_2$) per 10×10^6 cells and incubated on ice for 10 min. One microlitre of 10% NP-40 detergent per 10×10^6 cells was added and the cells were homogenized at 4°C with the tight pestle in a glass dounce homogenizer for at least 15 strokes. Nuclei were washed with 1 ml of cold RSB buffer and resuspended in 74.25 μl of 1× M. *Sss* I buffer+sucrose per 1×10^6 nuclei. 1×10^6 nuclei were treated with 60 units of M. *Sss* I (New England BioLabs, Inc., Beverly, MA, USA) in a final volume of 150 μl for 15 min at 37°C. M. *Sss* I treated purified control gDNA (6 μg) was used as a positive control. Reactions were stopped by the addition of an equal volume of stop solution (20 mM Tris–HCl; pH 7.9, 600 mM NaCl, 1% SDS and 10 mM EDTA) and proteinase K treatment for 48 h at 37°C. DNA was purified by phenol chloroform extraction, ethanol precipitated and resuspended in water. One microgram of sheared M. *Sss* I treated nuclei or control gDNA was bisulphite converted for 16 h at 55°C, under conditions previously described (48). After bisulphite conversion, the DNA was ethanol precipitated, dried, resuspended in 50 μl water and stored at −20°C. Bisulphite genomic sequencing was used to analyse the methylation status of individual molecules modified by M. *Sss* I across the three neighbouring regions of the $p16^{INK4A}$ CpG island associated promoter region described in Supplementary Material, Figure S1. Lowess curves were generated and smoothing applied over 10 data points in order to highlight similarities between the methylation patterns seen for the *in vitro* MSPA data with the *in vivo* Bre-38 post-selection methylation data.

Chromatin immunoprecipitation assays

Chromatin immunoprecipitation assays were carried out according to the manufacturer's instructions (Upstate/Millipore, Temecula, CA, USA) using pooled Bre-60 and Bre-70 pre-selection cedllsd, Bre-80 post-selection ceslls, Bre-12 pre- and post-selection cells, Bre-40 pre- and post-selection cells and Bre-38 pre- and post-selection cells, essentially as described (30). The eluted complexes were immunoprecipitated with antibodies specific for acetylated H3K9 (H3K9Ac, Upstate/Millipore), dimethylated H3K9 (H3K9Me2, Upstate/Millipore) and trimethylated H3K27 (H3K27Me3, Upstate/Millipore) and DNA yield was measured by quantitative real-time PCR as described (30). Chromatin immunoprecipitation amplification primers are described in Supplementary Material, Table S1.

SUPPLEMENTARY MATERIAL

Supplementary Material is available at *HMG* online.

ACKNOWLEDGEMENTS

We would like to thank Marcel Coolen for critical reading of the manuscript and help with figures, Christopher Molloy and Jane Noble for experimental assistance and Professors Thea Tlsty and Peter Jones for technical advice.

Conflict of Interest statement. None declared.

FUNDING

This work is supported by Cancer Institute NSW (CI NSW), National Breast Cancer Foundation (NBCF) and National Health and Medical Research Council (NH&MRC) project grants; Dora Lush Biomedical Postgraduate Scholarship from the NH&MRC, CI NSW Research Scholar Award and NBCF Excellence Award (R.A.H.); and NH&MRC fellowships (S.J.C. and R.R.R.).

REFERENCES

1. Kornberg, R.D. (1974) Chromatin structure: a repeating unit of histones and DNA. *Science*, **184**, 868–871.
2. Schones, D.E., Cui, K., Cuddapah, S., Roh, T.Y., Barski, A., Wang, Z., Wei, G. and Zhao, K. (2008) Dynamic regulation of nucleosome positioning in the human genome. *Cell*, **132**, 887–898.
3. Li, B., Carey, M. and Workman, J.L. (2007) The role of chromatin during transcription. *Cell*, **128**, 707–719.
4. Baylin, S.B., Esteller, M., Rountree, M.R., Bachman, K.E., Schuebel, K. and Herman, J.G. (2001) Aberrant patterns of DNA methylation, chromatin formation and gene expression in cancer. *Hum. Mol. Genet.*, **10**, 687–692.
5. Baylin, S.B. (2005) DNA methylation and gene silencing in cancer. *Nat. Clin. Pract. Oncol.*, **2** (Suppl 1.), S4–S11.
6. Jones, P.A. (2005) Overview of cancer epigenetics. *Semin. Hematol.*, **42**, S3–S8.
7. Gal-Yam, E.N., Saito, Y., Egger, G. and Jones, P.A. (2008) Cancer epigenetics: modifications, screening, and therapy. *Annu. Rev. Med.*, **59**, 267–280.
8. Gardiner-Garden, M. and Frommer, M. (1987) CpG islands in vertebrate genomes. *J. Mol. Biol.*, **196**, 261–282.
9. Bird, A.P. (1986) CpG-rich islands and the function of DNA methylation. *Nature*, **321**, 209–213.
10. Wong, D.J., Foster, S.A., Galloway, D.A. and Reid, B.J. (1999) Progressive region-specific de novo methylation of the p16 CpG island in primary human mammary epithelial cell strains during escape from M(0) growth arrest. *Mol. Cell. Biol.*, **19**, 5642–5651.

11. Clark, S.J. and Melki, J. (2002) DNA methylation and gene silencing in cancer: which is the guilty party? *Oncogene*, **21**, 5380–5387.
12. Sherr, C.J. (2001) The ink4a/arf network in tumour suppression. *Nat. Rev. Mol. Cell. Biol.*, **2**, 731–737.
13. Rocco, J.W. and Sidransky, D. (2001) p16(MTS-1/CDKN2/INK4a) in cancer progression. *Exp. Cell. Res.*, **264**, 42–55.
14. Herman, J.G. (1999) p16(INK4): involvement early and often in gastrointestinal malignancies. *Gastroenterology*, **116**, 483–485.
15. Belinsky, S.A., Nikula, K.J., Palmisano, W.A., Michels, R., Saccomanno, G., Gabrielson, E., Baylin, S.B. and Herman, J.G. (1998) Aberrant methylation of p16(INK4a) is an early event in lung cancer and a potential biomarker for early diagnosis. *Proc. Natl Acad. Sci. USA*, **95**, 11891–11896.
16. Nuovo, G.J., Plaia, T.W., Belinsky, S.A., Baylin, S.B. and Herman, J.G. (1999) In situ detection of the hypermethylation-induced inactivation of the p16 gene as an early event in oncogenesis. *Proc. Natl Acad. Sci. USA*, **96**, 12754–12759.
17. Noble, J.R., Rogan, E.M., Neumann, A.A., Maclean, K., Bryan, T.M. and Reddel, R.R. (1996) Association of extended in vitro proliferative potential with loss of p16INK4 expression. *Oncogene*, **13**, 1259–1268.
18. Foster, S.A., Wong, D.J., Barrett, M.T. and Galloway, D.A. (1998) Inactivation of p16 in human mammary epithelial cells by CpG island methylation. *Mol. Cell. Biol.*, **18**, 1793–1801.
19. Huschtscha, L.I., Noble, J.R., Neumann, A.A., Moy, E.L., Barry, P., Melki, J.R., Clark, S.J. and Reddel, R.R. (1998) Loss of p16INK4 expression by methylation is associated with lifespan extension of human mammary epithelial cells. *Cancer Res.*, **58**, 3508–3512.
20. Brenner, A.J., Stampfer, M.R. and Aldaz, C.M. (1998) Increased p16 expression with first senescence arrest in human mammary epithelial cells and extended growth capacity with p16 inactivation. *Oncogene*, **17**, 199–205.
21. Romanov, S.R., Kozakiewicz, B.K., Holst, C.R., Stampfer, M.R., Haupt, L.M. and Tlsty, T.D. (2001) Normal human mammary epithelial cells spontaneously escape senescence and acquire genomic changes. *Nature*, **409**, 633–637.
22. Holst, C.R., Nuovo, G.J., Esteller, M., Chew, K., Baylin, S.B., Herman, J.G. and Tlsty, T.D. (2003) Methylation of p16(INK4a) promoters occurs in vivo in histologically normal human mammary epithelia. *Cancer Res.*, **63**, 1596–1601.
23. Crawford, Y.G., Gauthier, M.L., Joubel, A., Mantei, K., Kozakiewicz, K., Afshari, C.A. and Tlsty, T.D. (2004) Histologically normal human mammary epithelia with silenced p16(INK4a) overexpress COX-2, promoting a premalignant program. *Cancer Cell*, **5**, 263–273.
24. Hammond, S.L., Ham, R.G. and Stampfer, M.R. (1984) Serum-free growth of human mammary epithelial cells: rapid clonal growth in defined medium and extended serial passage with pituitary extract. *Proc. Natl Acad. Sci. USA*, **81**, 5435–5439.
25. Stampfer, M.R. and Bartley, J.C. (1985) Induction of transformation and continuous cell lines from normal human mammary epithelial cells after exposure to benzo[a]pyrene. *Proc. Natl Acad. Sci. USA*, **82**, 2394–2398.
26. Sandhu, C., Donovan, J., Bhattacharya, N., Stampfer, M., Worland, P. and Slingerland, J. (2000) Reduction of Cdc25A contributes to cyclin E1-Cdk2 inhibition at senescence in human mammary epithelial cells. *Oncogene*, **19**, 5314–5323.
27. Stampfer, M.R., Yaswen, P., Casto, B.C. and Schuler, C.F. (1992) *Transformation of Human Epithelial Cells: Moleculare and Oncogene Mechanisms*. CRC Press Inc., Boca Raton.
28. Tlsty, T.D., Romanov, S.R., Kozakiewicz, B.K., Holst, C.R., Haupt, L.M. and Crawford, Y.G. (2001) Loss of chromosomal integrity in human mammary epithelial cells subsequent to escape from senescence. *J. Mammary Gland Biol. Neoplasia*, **6**, 235–243.
29. Tlsty, T.D., Crawford, Y.G., Holst, C.R., Fordyce, C.A., Zhang, J., McDermott, K., Kozakiewicz, K. and Gauthier, M.L. (2004) Genetic and epigenetic changes in mammary epithelial cells may mimic early events in carcinogenesis. *J. Mammary Gland Biol. Neoplasia*, **9**, 263–274.
30. Hinshelwood, R.A., Huschtscha, L.I., Melki, J., Stirzaker, C., Abdipranoto, A., Vissel, B., Ravasi, T., Wells, C.A., Hume, D.A., Reddel, R.R. *et al.* (2007) Concordant epigenetic silencing of transforming growth factor-beta signaling pathway genes occurs early in breast carcinogenesis. *Cancer Res.*, **67**, 11517–11527.
31. Fatemi, M., Pao, M.M., Jeong, S., Gal-Yam, E.N., Egger, G., Weisenberger, D.J. and Jones, P.A. (2005) Footprinting of mammalian promoters: use of a CpG DNA methyltransferase revealing nucleosome positions at a single molecule level. *Nucleic Acids Res.*, **33**, e176.
32. Kladde, M.P. and Simpson, R.T. (1996) Chromatin structure mapping *in vivo* using methyltransferases. *Methods Enzymol.*, **274**, 214–233.
33. Hinshelwood, R.A. and Clark, S.J. (2008) Breast cancer epigenetics: normal human mammary epithelial cells as a model system. *J. Mol. Med.*
34. Baylin, S. and Bestor, T.H. (2002) Altered methylation patterns in cancer cell genomes: cause or consequence? *Cancer Cell*, **1**, 299–305.
35. Bachman, K.E., Park, B.H., Rhee, I., Rajagopalan, H., Herman, J.G., Baylin, S.B., Kinzler, K.W. and Vogelstein, B. (2003) Histone modifications and silencing prior to DNA methylation of a tumor suppressor gene. *Cancer Cell*, **3**, 89–95.
36. Stein, R., Razin, A. and Cedar, H. (1982) In vitro methylation of the hamster adenine phosphoribosyltransferase gene inhibits its expression in mouse L cells. *Proc. Natl Acad. Sci. USA*, **79**, 3418–3422.
37. Busslinger, M., Hurst, J. and Flavell, R.A. (1983) DNA methylation and the regulation of globin gene expression. *Cell*, **34**, 197–206.
38. Yisraeli, J., Frank, D., Razin, A. and Cedar, H. (1988) Effect of in vitro DNA methylation on beta-globin gene expression. *Proc. Natl Acad. Sci. USA*, **85**, 4638–4642.
39. Stirzaker, C., Song, J.Z., Davidson, B. and Clark, S.J. (2004) Transcriptional gene silencing promotes DNA hypermethylation through a sequential change in chromatin modifications in cancer cells. *Cancer Res.*, **64**, 3871–3877.
40. Gal-Yam, E.N., Jeong, S., Tanay, A., Egger, G., Lee, A.S. and Jones, P.A. (2006) Constitutive nucleosome depletion and ordered factor assembly at the GRP78 promoter revealed by single molecule footprinting. *PLoS. Genet.*, **2**, e160.
41. Mito, Y., Henikoff, J.G. and Henikoff, S. (2005) Genome-scale profiling of histone H3.3 replacement patterns. *Nat. Genet.*, **37**, 1090–1097.
42. Lin, J.C., Jeong, S., Liang, G., Takai, D., Fatemi, M., Tsai, Y.C., Egger, G., Gal-Yam, E.N. and Jones, P.A. (2007) Role of nucleosomal occupancy in the epigenetic silencing of the MLH1 CpG island. *Cancer Cell*, **12**, 432–444.
43. Ohm, J.E., McGarvey, K.M., Yu, X., Cheng, L., Schuebel, K.E., Cope, L., Mohammad, H.P., Chen, W., Daniel, V.C., Yu, W. *et al.* (2007) A stem cell-like chromatin pattern may predispose tumor suppressor genes to DNA hypermethylation and heritable silencing. *Nat. Genet.*, **39**, 237–242.
44. Widschwendter, M., Fiegl, H., Egle, D., Mueller-Holzner, E., Spizzo, G., Marth, C., Weisenberger, D.J., Campan, M., Young, J., Jacobs, I. *et al.* (2007) Epigenetic stem cell signature in cancer. *Nat. Genet.*, **39**, 157–158.
45. Huschtscha, L.I., Neumann, A.A., Noble, J.R. and Reddel, R.R. (2001) Effects of simian virus 40 T-antigens on normal human mammary epithelial cells reveal evidence for spontaneous alterations in addition to loss of p16(INK4a) expression. *Exp. Cell. Res.*, **265**, 125–134.
46. Millar, D.S., Warnecke, P.M., Melki, J.R. and Clark, S.J. (2002) Methylation sequencing from limiting DNA: embryonic, fixed, and microdissected cells. *Methods*, **27**, 108–113.
47. Micke, P., Ostman, A., Lundeberg, J. and Ponten, F. (2005) Laser-assisted cell microdissection using the PALM system. *Methods Mol. Biol.*, **293**, 151–166.
48. Clark, S.J., Harrison, J., Paul, C.L. and Frommer, M. (1994) High sensitivity mapping of methylated cytosines. *Nucleic Acids Res.*, **22**, 2990–2997.
49. Clark, S.J., Statham, A., Stirzaker, C., Molloy, P.L. and Frommer, M. (2006) DNA methylation: bisulphite modification and analysis. *Nat. Protoc.*, **1**, 2353–2364.
50. Frigola, J., Song, J., Stirzaker, C., Hinshelwood, R.A., Peinado, M.A. and Clark, S.J. (2006) Epigenetic remodeling in colorectal cancer results in coordinate gene suppression across an entire chromosome band. *Nat. Genet.*, **38**, 540–549.